DOI: 10.1002/adma.200701297

Galvanic Replacement Reaction on Metal Films: A One-Step Approach to Create Nanoporous Surfaces for Catalysis**

By *Vipul Bansal*, *Harit Jani*, *Johan Du Plessis*, *Peter J. Coloe*, and *Suresh K. Bhargava**

Porous materials are of great interest because of their interesting structural, optical and surface properties, leading to a wide range of applications.[1,2] Among the various properties of porous materials, their high specific surface area, low density, and cost-effectiveness are particularly notable and make them attractive candidates for catalysis,[3] sensing[4] and actuation[5] applications. Nanoporous particles in particular are attractive candidates for these applications, because of their higher surface-to-volume ratio in comparison with bulk counterparts. There have been numerous efforts towards the solution-based synthesis of porous and hollow metal nanoparticles,[6–10] however their applicability is limited as the assembly of individual nanoparticles present in solution is still a major challenge. There have also been limited efforts towards the creation of porosity in thin films.[11] Most of the efforts in this direction have been limited to the de-alloying process, in which one of the components of an alloy is selectively dissolved using an acid, leaving behind a porous network/channel of the more noble metal component.[11,12] However, the acid-mediated de-alloying process requires the cumbersome task of alloy formation and has limited applicability to those metal alloy systems wherein both of the metal components dissolve into the de-alloying solution (acid). This therefore necessitates the use of a different approach for the creation of porosity in supported metal thin films and/or metal foils, which can be universally applied to all the metallic systems.

Recently, galvanic replacement reactions (transmetallation reactions) involving sacrificial metal nanoparticles and suitable metal ions have been employed by various groups[13–18] for the synthesis of hollow/porous metal[13,14] and metal alloy[15,16] nanostructures in aqueous[14–17] and organic environments.[18] Galvanic replacement reactions are single-step reactions that utilize the differences in the standard electrode potentials of various elements, leading to deposition of the more noble element and dissolution of the less noble component. The electroless nature of galvanic replacement reactions provides them the unique and significant advantage of simplicity. Very recently, the potential of galvanic replacement reactions was also explored for the epitaxial growth of thin films.[19]

In this study, we have investigated the scope of galvanic replacement reactions as a versatile tool for the creation of nanoscale porosity in metal foils as a representative of bulk metal surfaces. More specifically, the reaction of Cu^{2+} ions with nickel foil results in a Cu-Ni nanoporous surface. The Cu-Ni nanoporous material has been characterized by using various microscopy tools including scanning electron microscopy (SEM), transmission electron microscopy (TEM), and Auger microscopy in addition to X-ray diffraction (XRD) and X-ray photoemission spectroscopy (XPS) analysis. Recognizing that such nanoporous surfaces would have a significantly enhanced surface area and surface defect sites relative to their solid counterparts, we show that these nanoporous surfaces are excellent candidates for catalysis applications. The applicability of highly porous Cu on nickel foil has been demonstrated in the catalytic wet air oxidation (CWAO) of ferulic acid (4-hydroxy-3-methoxycinnamic acid), a model organic compound obtained by the degradation of lignin in pulp mill effluents.[20] Ferulic acid contains the guaiacol moiety prominent in both hardwood and softwood lignin as well as a propenyl substituent similar to that found in various linkages between lignin constituents, which are extremely difficult to oxidize under ambient conditions and pose a major threat to water reservoirs.[21] Our studies indicate that a nanoporous Cu-Ni catalyst is able to oxidize ferulic acid under significantly milder conditions than conventional wet air oxidation processes.

The Cu-Ni nanocatalyst prepared using transmetallation reaction was analyzed using SEM. Figure 1A shows the representative SEM image recorded from nickel foil before its reaction with Cu^{2+} ions. The SEM image clearly indicates a relatively flat surface of the nickel foil used to prepare the cat-

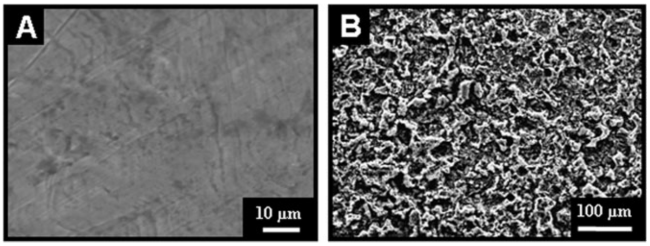

Figure 1. SEM images showing the surface of the nickel foil A) before, and B) after its reaction with Cu^{2+} ions for 30 min.

---

[*] Dr. S. K. Bhargava, V. Bansal, H. Jani, J. Du Plessis, P. J. Coloe
School of Applied Sciences
RMIT University
GPO Box 2476V, Melbourne, VIC 3001 (Australia)
E-mail: suresh.bhargava@rmit.edu.au

[**] V.B. thanks the Australian Research Council for ARC-International Visiting Research Fellowship. The authors thank Mr. Desmond Lau for assistance with EDX and EELS measurements. Supporting Information is available online from Wiley InterScience or from the authors.

WILEY InterScience® DISCOVER SOMETHING GREAT

alyst for this study (Fig. 1A). Figure 1B shows a representative SEM image of the nickel surface after its reaction with Cu^{2+} ions for 30 min. It is evident from the SEM images (Fig. 1) that the reaction of nickel metal with Cu^{2+} ions results in a network-like highly porous nickel surface as a result of the kinetically favorable replacement reaction between Ni^0 and Cu^{2+}. Galvanic replacement reactions operate on the basis of differences in the standard reduction potential of the systems under investigation. Since the standard reduction potential of the Cu^{2+}/Cu pair (+0.34 V wrt. standard hydrogen electrode (SHE)) is higher than that of the Ni^{2+}/Ni pair (–0.25 V wrt. SHE), nickel membrane in aqueous solution can be oxidized by $CuCl_2$ according to the following replacement reaction:

$$Ni_{(s)}{}^0 + Cu^{2+}{}_{(aq)} \rightarrow Cu_{(s)}{}^0 + Ni^{2+}{}_{(aq)}$$

The oxidation of $Ni^0{}_{(s)}$ into $Ni^{2+}{}_{(aq)}$ ions leads to its leaching in the surrounding aqueous environment and elemental copper (Cu^0) is simultaneously produced, which is deposited onto nickel foil. In the current system of interest (Cu-Ni), where displacing and sacrificing metals manifest equal oxidation states (2:2), the odds to obtain a layer that perfectly reproduces the substrate morphology are substantially higher. Apparently, we should ideally expect to obtain an ideal layer-by-layer replacement growth of Cu on Ni.[19] In our view, such growth does take place to a large extent in these experiments. However, a departure from ideality is expected owing to the atomic size difference between the deposited and sacrificial metal, the roughness of the Ni foil used as a sacrificial metal, and also because of the fact that stoichiometric redox exchange is initialized mainly on the flat terraces (it is easier to replace an atom from a terrace site than from a step and/or kink site).[22] Following these discussions, it is highly possible that the galvanic replacement reaction on rough nickel foil would lead to the deposition of elemental Cu at various nucleation sites in the form of nanoparticles. Moreover, the continuous diffusion of Cu^{2+} as well as Ni^{2+} ions during the reaction would eventually lead to deeply inherited nanoporous Cu structures on the sacrificial Ni surface until the nickel template is completely consumed.

In order to understand the implications of the transmetallation reaction in the Cu-Ni system and to further determine the level of porosity achieved, the Cu-Ni foil obtained after the transmetallation reaction was subjected to ultrasonication in water for 1 h and the solution obtained thereafter was subjected to TEM measurements. Figure 2 shows representative TEM images of the Cu-Ni hybrid structures separated from the nickel foil during ultrasonication. The TEM images clearly indicate the formation of sievelike porous structures as a result of the transmetallation reaction (Fig. 2A and B).

The higher magnification TEM image (inset Fig. 2B) clearly indicates the formation of honeycomb structures with pores and particles ranging in sub-5 nm size regime. We believe that in principle, atomic-scale porosity can be achieved using transmetallation reaction since these reactions progress at such scales; however, it is beyond the resolution limit of the instrument used here for analysis. High resolution TEM (HRTEM) measurements on these samples are under investigation, and should provide a detailed understanding of the underlying phenomenon. In addition, it also appears from these honeycomb structures that the porosity is not limited to the surface but is deeply inherited, making the nickel foil highly porous and hence significantly enhancing the overall porosity.

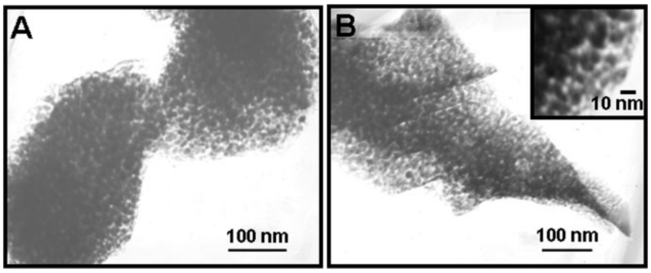

Figure 2. TEM images showing the Cu-Ni nanocatalyst surface after 4 h of galvanic replacement reaction. The inset in (B) shows the honeycomb structures observed during the higher-magnification imaging.

Important information about the transmetallation process can be obtained by recording the changes in the surface features of the Cu-Ni system during a time-dependent transmetallation reaction experiment. Figure 3 shows the representative SEM images of Cu-Ni system obtained after reaction of nickel foil with Cu^{2+} ions for 30 min (A and B), 1 h (C and D), 2 h (E and F), 4 h (G and H), and 8 h (I and J), respectively. It is clear from the SEM images that nickel foil becomes highly rough and porous after reaction with Cu^{2+} for 30 min (Fig. 3A and B) when compared to its surface before reaction (Fig. 1A). As the reaction proceeds, the Cu^{2+} ions begin to penetrate through the preformed pores, leading to hollow/porous ball-like structures within 1 h (Fig. 3C), which on higher magnification appear to consist of flakes (Fig. 3D). When the reaction between nickel foil and Cu^{2+} ions is continued for 2 h, the Cu^{2+} ions begin to react with preformed flakes, leading to formation of rosettelike structures after 2 h of reaction (Fig. 3E and F). On further exposure to Cu^{2+} ions until 4 h, these rosette structures break apart into smaller perforated balls (Fig. 3G and H). These micrometer-sized balls further break open in 8 h, leading to overlaying flat Cu-Ni networks consisting of nanowires- and nanoribbon-like structures (Fig. 3I and J). Although, SEM imaging only records the changes in surface morphology of nickel foil during the transmetallation reaction, from the time-dependent SEM analysis it appears that the underlying layers of nickel foil are continuously exposed to fresh Cu^{2+} ions, leading to the creation of enhanced porosity, the enhancement of the surface area, and the deposition of more Cu in the nickel foil (Fig. 3A–J). This is also evident by cross-sectional SEM imaging of Ni foil obtained by transmetallation reaction with Cu^{2+} ions for 4 h, which in fact suggests that deeply inherited nanoporous structures can be created using transmetallation reactions (Supporting Information, Fig. S1). Thus, SEM imaging suggests a

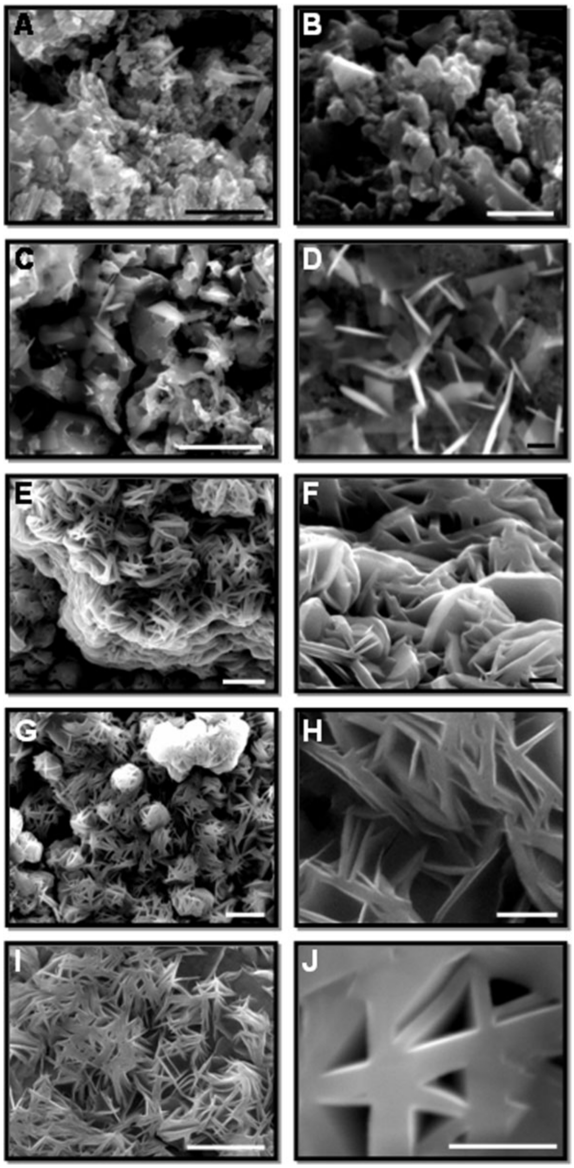

Figure 3. SEM images showing the Cu-Ni nanocatalyst surface after A,B) 30 min, C,D) 1 h, E,F) 2 h, G,H) 4 h, and I,J) 8 h of galvanic replacement reaction. Scale bars in first and second columns correspond to 5 µm and 1 µm, respectively.

remarkable ability to tune the bulk surfaces by the proposed galvanic replacement approach.

In order to determine the nature of metal phases formed during galvanic replacement reaction as well as reveal any Cu-Ni synergism, the nickel foil was subjected to XRD measurements before (curve 1, Fig. 4) and after the transmetallation reaction (curve 2, Fig. 4). The XRD pattern of nickel foil (curve 1) shows the presence of well-defined Bragg reflections, which could be indexed based on the structure of metallic nickel.[23] After the transmetallation reaction with Cu^{2+} ions (curve 2), additional Bragg reflections were observed that could be collectively assigned to copper oxide and nickel oxide.[24] In addition, a shift in the Ni peaks towards lower 2θ values was observed. The fact that both Ni and Cu have fcc structures with very similar lattice parameters of 3.51 and 3.66 Å [Ni: 2θ = 44.5°, 51.8°, and 76.4°; Cu: 2θ = 44.3°, 50.4°, and 74.1°] makes it difficult to assign the peaks unequivocally to Cu/Ni, however after the transmetallation reaction a shift in Ni peaks towards Cu was observed, which indicates the formation of Cu nanoparticles. Additionally, peak broadening was also observed, which indicates the formation of nanocrystalline copper/copper oxide as a result of the transmetallation reaction. Although transmetallation of Ni with Cu^{2+} ions is expected to create metallic Cu in the vicinity of nickel foil, the possibility of the further oxidation of copper in an aqueous environment, leading to the formation of porous copper oxide nanostructures embedded in Ni foil, can not be ignored.

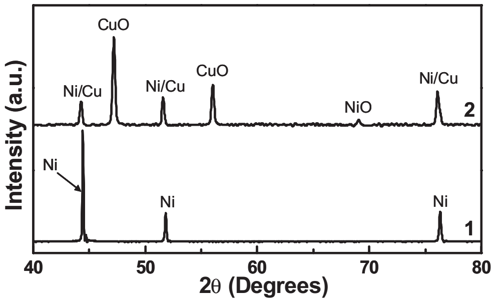

Figure 4. XRD patterns obtained from Ni foil before (curve 1) and after (curve 2) its transmetallation reaction with Cu^{2+} ions.

The catalyst surface plays the key role in the catalytic reactions, and the composition of the surface may not be the same as the bulk catalytic system used in this study. Therefore the chemical surface analysis of Cu-Ni catalyst used in this study was performed using XPS, which is a highly surface sensitive technique (Fig. 5). Figure 5A shows the Ni $2p_{3/2}$ XPS spectra before (curve 1) and after (curve 2) the galvanic replacement

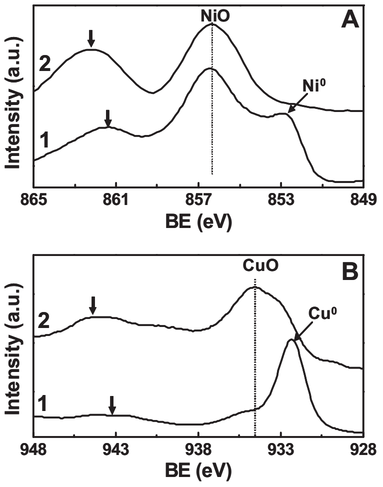

Figure 5. XPS spectra showing A) $Ni2p_{3/2}$ core levels in Ni foil before (curve 1) and after (curve 2) the galvanic replacement reaction. B) $Cu2p_{3/2}$ core levels in Cu-Ni catalyst before (curve 1) and after CWAO process (curve 2). The satellite peaks in the above spectra have been indicated by arrow marks.

reaction with Cu^{2+} ions. Before the transmetallation reaction, the Ni 2p core level spectrum shows two major $2p_{3/2}$ components at ca. 852.9 eV and 856.5 eV, which can be assigned to Ni^0 and NiO respectively (curve 1, Fig. 5A).[25] The simultaneous presence of Ni and NiO components indicates the partial oxidation of Ni foil surface on its exposure to air. Apart from these two components, a weak satellite peak towards higher BE was also observed in the unreacted Ni sample (curve 1, Fig. 5A). On the other hand, after exposure of nickel foil to Cu^{2+} ions, we observed that the Ni^0 peak vanished completely with the development of a more pronounced NiO peak, indicating that Ni surface has oxidized to NiO during transmetallation in the aqueous environment (curve 2, Fig. 5A). The XPS results correlate well with the XRD data, which also show the presence of NiO peaks (curve 2, Fig. 4). Additionally, it should be noted that the shake-up satellites in the Ni $2p_{3/2}$ XPS spectrum become more intense after the replacement reaction (compare curve 2 and curve 1 in Fig. 5A). Since the shake-up satellites are mainly 3d → 4s transitions which are forbidden in metals but present in transition metal oxides, the oxidation of Ni to NiO increases the intensity of these satellites.[25]

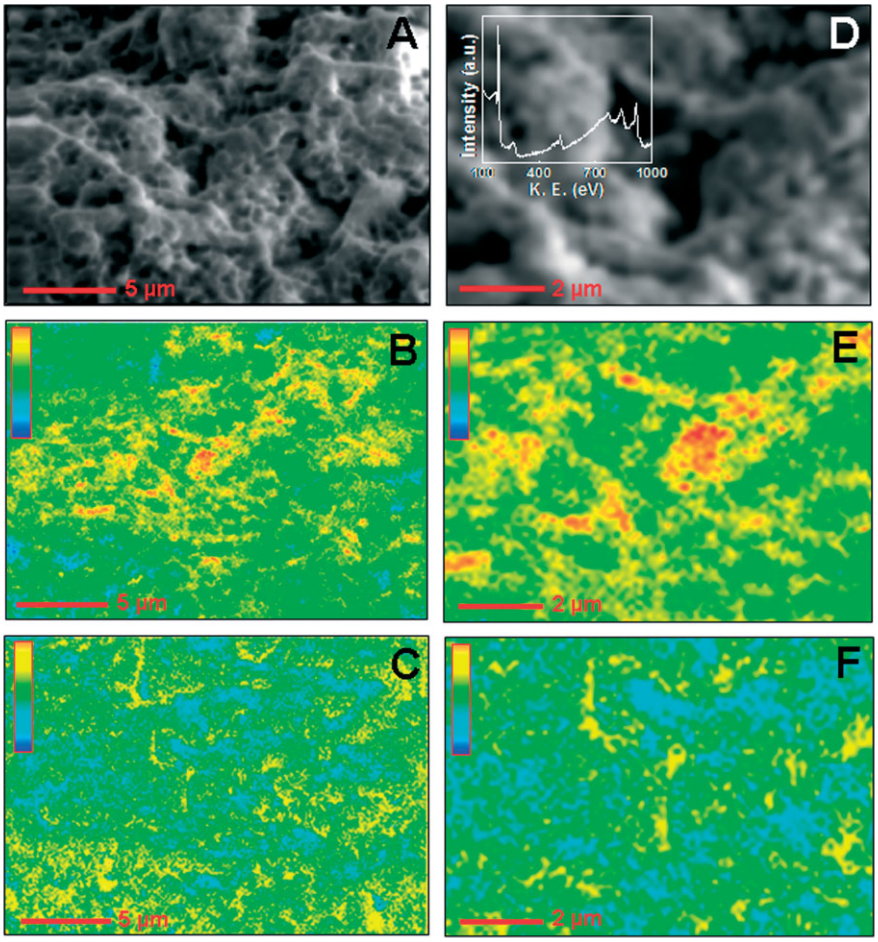

Figure 6. Auger microscopy data on Cu-Ni nanocatalyst surface showing A–C) lower- and D–F) higher-magnification images while scanned for SEM imaging (A and D), Cu LMM signal (B and E) and Ni LMM signal (C and F), respectively. The inset in D shows the AES spectrum obtained from Cu-Ni surface.

When the Cu-Ni sample obtained after the transmetallation reaction was scanned for $Cu2p_{3/2}$ core levels, a strong BE component at ca. 932.3 eV along with a shoulder towards higher BE was observed (curve 1, Fig. 5B). The main component at ca. 932.3 eV corresponds to Cu^0, while the presence of the weak shoulder towards higher BE at ca. 934.5 eV indicates that some Cu^0 was oxidized to CuO in aqueous solution during the transmetallation reaction.[25] The presence of Cu^0 further supports our TEM (Fig. 2), SEM (Fig. 3), and XRD (Fig. 4) observations, wherein Cu nanoparticles formed during the replacement reaction were found to be deeply embedded in nickel foil.

Once the formation of Cu nanoparticles in Ni foil was established by XRD and XPS measurements, SEM coupled with Auger imaging and Auger electron spectroscopy (AES) were performed on the Cu-Ni surface to further understand the distribution of Cu particles on the surface of Ni foil (Fig. 6). The inset in Figure 6D shows the AES spectrum of the surface of Cu-Ni catalyst, showing Cu LMM and Ni NLL Auger peaks at 916 eV and 844 eV kinetic energies (K.E.) respectively, which were employed for Auger imaging.

In Auger imaging, hot colors, such as bright and red colors, represent a high concentration of the examined elements (Cu and Ni in this case) while cold colors, such as green and cyan, represent a low concentration of the examined elements. By inspection of the lower- (Fig. 6B and C) and higher-magnification (Fig. 6E and F) Auger images of Cu-Ni sample, it can be seen that though Cu and Ni are reasonably well-distributed throughout the sample, the Auger images of Cu (Fig. 6B and E) show more brighter spots/clusters (red and yellow colors) than those of Ni (Fig. 6C and F). This indicates that the etching of the sacrificial Ni surface initially begins uniformly on the Ni foil, however as the transmetallation reaction proceeds with time, more defect sites are created, which assist in further facile effusion of the oxidized Ni^{2+} ions from these sites and hence result in further nucleation of Cu nanoparticles closer to those sites. These speculations are supported by previous high-resolution TEM measurements in Au-Ag systems, wherein Shukla and co-workers highlighted the important role that defect sites and twin boundaries can play during transmetallation reactions.[17] It is important to note that chemical mapping in Cu-Ni system in order to understand the distribution of Cu and Ni local phases using TEM coupled with EDS (energy-dispersive X-ray spectroscopy) and/or EELS (electron energy-loss spectroscopy) were not particularly advantageous, because of significant overlap of Cu and Ni spectral lines during EDS[26] and EELS.[27] Additionally, the contamination of Cu signals arising from Cu TEM grids further complicates the imaging of Cu phases in Cu-Ni system. Therefore, AES microscopy was performed to understand the distribution of Cu and Ni phases in Cu-Ni system.

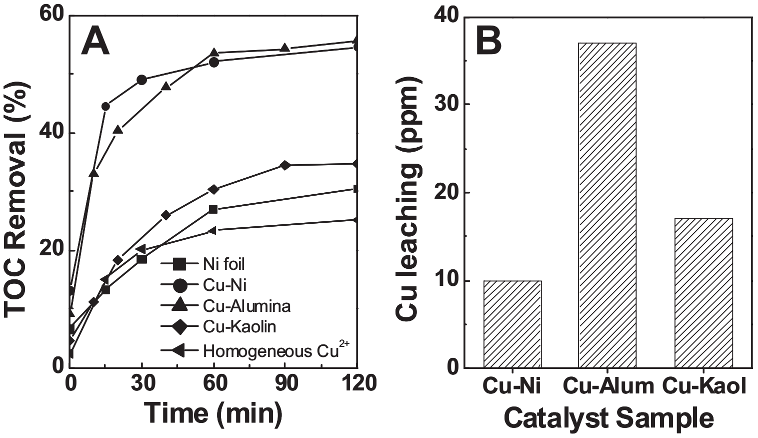

Figure 7. A) Total organic carbon (TOC) data showing the efficiency of various Cu-based catalysts for removal of organic carbon during CWAO of ferulic acid. B) ICP-MS data showing Cu leaching from various catalysts during CWAO of ferulic acid for 2 h.

The understanding of the Cu-Ni interactions supported by the SEM, TEM, XRD, XPS, and AES results motivated us to explore the catalytic activity of the highly porous Cu-Ni heterogeneous nanocomposite in CWAO of ferulic acid, a model lignin compound found in waste from paper and pulp mill effluents. Lignin and related compounds are known to be extremely difficult to oxidize, especially under mild temperature and pressure conditions, and pose a major threat to water reservoirs.[21] We observed that the Cu-Ni nanocatalyst could oxidize more than 45 % of ferulic acid at 100 °C within 15 min, while the Ni foil could oxidize only 12 % of ferulic acid within the same period (Fig. 7A). In order to compare the Cu-Ni catalyst formed by the transmetallation reaction with the conventional Cu-based catalysts, high surface area catalysts (Cu-Alumina and Cu-Kaolin) were synthesized using ion-impregnation method.[28] As is evident from Figure 7A, Cu-Kaolin and Cu-Alumina synthesized by conventional methods show much lesser oxidative activity (11 % and 32 % respectively in 15 min) in comparison with a Cu-Ni catalyst synthesized by the galvanic replacement method (45 % in 15 min). The higher oxidative activity of the Cu-Ni nanocatalyst can be attributed to the atomic-level porosity and the high number of defect sites in the Cu-Ni catalyst generated as a result of replacement reaction.

It is interesting to note that after 1 h of reaction, the oxidative activity of the Cu-Ni catalyst was stabilized at 55 %. Similarly, the activity of the Cu-Alumina catalyst also stabilizes at the same level after longer exposure time. The stabilization of the catalytic oxidation of ferulic acid beyond this point, even after longer hours of exposure to the catalyst (2 h) at 100 °C, can be attributed to the formation of low-molecular-weight acids and other degradation products during the CWAO process that are known to be extremely resistant to CWAO under the conditions used in this study.[29,30] Our preliminary results with Fourier-transform infrared spectroscopy (FT-IR) and gas chromatography-mass spectroscopy (GC-MS) indicate the formation of similar compounds including formic acid, 2-methoxy-4-vinylphenol and vanillin, which are generally known to require considerably harsher conditions for catalytic oxidation (Scheme 1).[29]

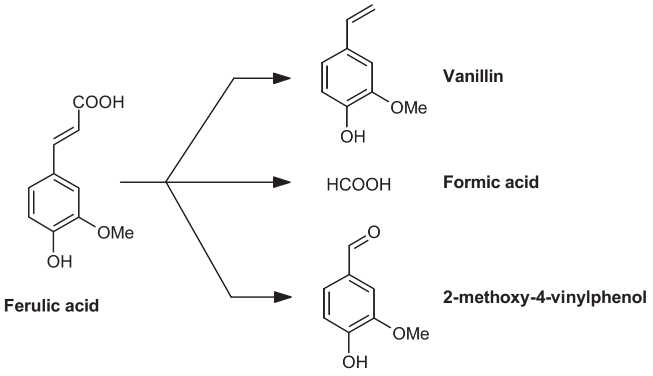

Scheme 1. Reaction scheme showing different products formed during CWAO of ferulic acid using Cu-Ni catalyst.

One of the important parameters in determining the feasibility of metal-based catalysts for the oxidation of industrial organic wastes is the amount of metal that is leached out during CWAO of organic wastes. This is becoming increasingly important due to the metal toxicity threats to our ecosystems. Moreover, the fact that the Cu-based catalysts are known to leach significantly during the CWAO process makes it even more important to minimize Cu leaching during CWAO.[31] Interestingly, ICP-MS results show that only 10 ppm of Cu is leached even after 2 h of CWAO, and the amount of Ni leached was negligible (Fig. 7B). On the other hand, Cu-alumina and Cu-kaolin catalysts prepared by conventional methods show higher Cu leaching of 37 ppm and 17 ppm, respectively, during CWAO of ferulic acid. The significant reduction in Cu leaching in the case of Cu-Ni catalyst might be due to the galvanic replacement method employed to prepare the Cu-Ni catalyst used in this study. During the galvanic replacement reaction, the Cu^{2+} ions replace Ni atoms from the nickel foil and Cu atoms simultaneously get chemically embedded into nickel foil, which might reduce Cu leaching. It is also possible that only certain crystallographic planes of Cu and certain defect sites are exposed and, hence, result in reduced leaching.

Though few studies in the literature deal with role of various crystallographic planes in different catalysis applications,[32,33] to our knowledge, there is no such study in CWAO process. A detailed understanding of the Cu leaching process can be obtained by similar studies. Our future efforts in this direction would involve an in-depth understanding of defect sites and crystallographic parameters and their role in CWAO of ferulic acid. Additionally, in order to verify the role of leached out Cu in CWAO of ferulic acid, 10 ppm of homogeneous Cu ($CuCl_2$) was used for CWAO of ferulic acid, which shows a much lower oxidation activity (Fig. 7A).

In this Communication, we have proposed a simple and generalized protocol for the creation of nanoscale porosity in bulk surfaces. The transmetallation (galvanic replacement) reaction based approach has been demonstrated to create a highly porous and active Cu-Ni heterogeneous catalyst. The applicability of the Cu-Ni nanocatalyst has been shown in terms of the degradation of ferulic acid, a model lignin compound found in pulp and paper mill effluents. It is particularly gratifying that the Cu-Ni nanocatalyst is active under moderate CWAO conditions, with significant reduction in metal leaching during oxidation. The simple concept of transmetallation reactions can be further utilized to tailor-design highly porous and active surfaces for catalysis and sensing applications. The vast commercial implications of transmetallation reactions for the large-scale synthesis of functional nanomaterials can not be overemphasized.

Experimental

Nickel foil (1 × 4 cm^2) was placed in a dialysis bag (12 kDa cut-off) containing 20 mL of deionized water (Milli-Q, Elix 3) and dialyzed against 100 mL of $CuCl_2$ (1 M) under constant stirring at room temperature for various time intervals (30 min, 1 h, 2 h, 4 h, and 8 h). The nickel foils obtained after galvanic replacement reactions were thoroughly washed with deionized water and dried under nitrogen. The confinement of nickel foil in the dialysis bag assisted in the controlled inward movement of Cu^{2+} ions to react slowly with nickel foil, as well as simultaneous outward movement of leached Ni^{2+} ions. Nickel foils before and after the reaction with Cu^{2+} ions for various time intervals (30 min, 1 h, 2 h, 4 h, and 8 h) were observed by SEM. SEM measurements were performed on a Philips XL30 SEM instrument operated at an accelerating voltage of 30 kV. For TEM measurements, nickel foil obtained after 4 h of galvanic replacement reaction was ultrasonicated in 5 mL of water for 1 h. Samples for TEM analysis were prepared by drop-coating the sonicated solutions on carbon-coated copper grids. TEM measurements were performed using a JEOL 1010 TEM instrument operated at an accelerated voltage of 100 kV. XRD measurements of nickel foil before and after reaction with Cu^{2+} ions were carried out on a Bruker D8 Advance XRD instrument operated at a voltage of 50 kV and a current of 35 mA with Cu Kα radiation. XPS measurements of Ni foil before and after reaction with Cu^{2+} ions as well as after reaction of the Cu-Ni catalyst with ferulic acid for 2 h were carried out on a VG MicroTech ESCA 310F instrument at a pressure better than 1×10^{-9} Torr (1 Torr = 1.333×10^2 Pa). The general scan and C 1s, Ni 2p, and Cu 2p core level spectra for the respective samples were recorded with un-monochromatized Mg Kα radiation (photon energy = 1253.6 eV) at a pass energy of 20 eV and electron takeoff angle (angle between electron emission direction and surface plane) of 90°. The core level binding energies (BEs) were aligned with the adventitious carbon binding energy of 285 eV.

In a typical catalysis experiment, 4 cm^2 of nickel foil before and after reaction with Cu^{2+} ions was used as catalyst at a pH range of 4–5. The high pressure and high temperature batch autoclave reactor was purchased from Parr Autoclaves, USA. All the catalysis experiments were carried out with 400 mL ferulic acid solution (1000 ppm) in a 1.2 L autoclave with a glass liner inside the reactor in order to avoid the leaching and contamination from the metal reactor wall. The stirring speed was constant (800 rpm) for all the experiments. Oxygen was introduced to the reactor after heating the ferulic acid to 100 °C in a nitrogen environment. The oxygen partial pressure input at ambient temperature was kept constant at 25 psi (1 psi = 6.895×10^3 Pa) for all experiments, which corresponds to 42 psi total pressure at 100 °C. The total organic carbon (TOC) concentration after the CWAO process was analyzed using an O. I. Analytical Model 1010 (USA) total carbon analyzer. TOC analysis of the oxidized product was performed in order to determine the amount of organic carbon remaining in solution after the CWAO process. The amount of Cu leaching during the CWAO process was determined using inductively coupled plasma-mass spectroscopy (ICP-MS) measurements. ICP-MS measurements were performed using HP4500 series 300, ShieldTorch System ICP-MS instrument. The supported Cu-Ni nanocatalyst prepared in this study by the galvanic replacement reaction was compared with conventional high surface area copper based catalysts as well as homogeneous Cu^{2+} ions. The conventional heterogeneous catalysts used in this study (Cu-Alumina and Cu-Kaolin) were prepared by ion-impregnation method, as described in our previous studies [28]. $CuCl_2$ was used as the homogeneous catalyst for CWAO studies. The catalysts used in control reactions were also analyzed using TOC and ICP-MS studies and compared with the Cu-Ni catalyst prepared by the transmetallation reaction.

Received: May 29, 2007
Revised: September 16, 2007
Published online: January 29, 2008

---

[1] D. L. Wilcox, M. Berg, T. Bernat, D. Kellerman, J. K. Cochran, in *MRS Symp. Proceedings*, Vol. 372, Materials Research Society, Pittsburgh, PA **1995**.
[2] F. Caruso, *Adv. Mater.* **2001**, *13*, 11.
[3] S. W. Kim, M. Kim, W. Y. Lee, T. Hyeon, *J. Am. Chem. Soc.* **2002**, *124*, 7642.
[4] M. Heida, R. Garcia, M. Dixon, T. Daniel, D. Allara, M. H. W. Chan, *Appl. Phys. Lett.* **2004**, *84*, 628.
[5] D. Kramer, R. N. Viswanath, J. Weissmuller, *Nano Lett.* **2004**, *4*, 793.
[6] S. Chah, J. H. Fendler, J. J. Yi, *J. Colloid Interface Sci.* **2002**, *250*, 142.
[7] F. Caruso, R. A. Caruso, H. Mohwald, *Science* **1998**, *282*, 1111.
[8] F. Caruso, M. Spasova, V. Maceira, L. M. Marzan, *Adv. Mater.* **2001**, *13*, 1090.
[9] S. J. Oldenburg, R. D. Averitt, S. L. Westcott, N. J. Halas, *Chem. Phys. Lett.* **1998**, *288–248*, 243.
[10] N. A. Dhas, K. S. Suslick, *J. Am. Chem. Soc.* **2005**, *127*, 2368.
[11] X. Lu, E. Bischoff, R. Spolenak, T. J. Balk, *Scr. Mater.* **2007**, *56*, 557.
[12] D. V. Pugh, A. Dursun, S. G. Corcoran, *J. Mater. Res.* **2003**, *18*, 216.
[13] Y. Sun, B. T. Mayers, Y. Xia, *Nano Lett.* **2002**, *2*, 481.
[14] Y. Sun, Y. Xia, *J. Am. Chem. Soc.* **2004**, *126*, 3892.
[15] H. Liang, Y. Guo, H. Zhang, J. Hu, J. Wan, C. L. Bai, *Chem. Commun.* **2004**, 1496.
[16] H. P. Liang, L. J. Wan, C. L. Bai, L. Jiang, *J. Phys. Chem. B* **2005**, *109*, 7795.
[17] S. Shukla, A. Priscilla, M. Banerjee, R. R. Bhonde, J. Ghatak, P. V. Satyam, M. Sastry, *Chem. Mater.* **2005**, *17*, 5000.
[18] P. R. Selvakannan, M. Sastry, *Chem. Commun.* **2005**, 1684.
[19] L. T. Viyannalage, R. Vasilic, N. Dimitrov, *J. Phys. Chem. C* **2007**, *111*, 4036.
[20] D. J. Conrad, P. M. Huck, *Water Res.* **1996**, *30*, 2776.

[21] M. Kindsigo, M. Hauteniemi, J. Kallas, *Wet Oxidation of Recalcitrant Lignin Water Solutions: Experimental and Reaction Kinetics*, Environmental Applications of Advanced Oxidation Processes (EAAOP), Chania **2006**, p. 203.

[22] E. B. Budevski, G. T. Staikov, W. J. Lorenz, *Electrochemical Phase Formation and Growth*, Wiley-VCH, Weinheim, Germany **1996**.

[23] A. R. Naghash, T. H. Etsell, S. Xu, *Chem. Mater.* **2006**, *18*, 2480.

[24] A. Hornes, D. Gamarra, G. Munuera, J. C. Conesa, A. M. Arias, *J. Power Sources* **2007**, *169*, 9.

[25] L. Fiermans, R. Hoogewijs, J. Vennik, *Surf. Sci.* **1975**, *47*, 1.

[26] I. P. Jones, in *Chemical Microanalysis Using Electron Beams*, The Institute of Materials, London **1992**.

[27] R. F. Egerton, in *Electron Energy-Loss Spectroscopy in the Electron Microscope*, Plenum, New York **1996**.

[28] S. K. Bhargava, H. Jani, J. Tardio, D. B. Akolekar, M. Hoang, *Ind. Eng. Chem. Res.* **2007**, *46*, 8652.

[29] S. K. Bhargava, J. Tardio, J. Prasad, K. Foger, D. B. Akolekar, S. C. Grocott, *Ind. Eng. Chem. Res.* **2006**, *45*, 1221.

[30] V. S. Mishra, V. V. Mahajani, J. B. Joshi, *Ind. Eng. Chem. Res.* **1995**, *34*, 2.

[31] A. Santos, P. Yustos, A. Quintanilla, G. Ruiz, F. Garcia-Ochoa, *Appl. Catal. B* **2005**, *61*, 323.

[32] R. Gomez, J. M. Orts, B. A. Ruiz, J. M. Feliu, *J. Phys. Chem. B* **2004**, *108*, 228.

[33] R. Narayanan, M. A. El-Sayed, *J. Phys. Chem. B* **2005**, *109*, 12663.